Henry Andrés PORRAS PERUCHO (ID)
Cláudio Manuel Vianna MOREIRA (ID)
Łukasz BORUC (ID)
Joanna GROCHOWALSKA (ID)
Łukasz Jan KAPUSTA (ID)

Combustion Engines
Polish Scientific Society of Combustion Engines

Spray structures formed by a multi-nozzle injector during the injection of a multi-component surrogate synthetic fuel under flash-boiling conditions

The introduction of synthetic fuels into spark-ignition direct-injection engines requires a deeper understanding of the injection and spray formation process. It also includes spray formation under flash-boiling conditions, which has not been of primary importance so far. This research focuses on experimental studies of spray propagation and its morphological features when moderate flash boiling is achieved. Our main objective is to verify this effect in a multiple-nozzle injection system for a selected synthetic fuel. It is accomplished by increasing the fuel temperature. The results showed that the spray structure changed slightly due to flash-boiling, but the secondary effects related to the rapid vaporisation of the injected fuel, such as spray collapse, were not observed.

1. Introduction

Due to the tightening of global regulations aimed at reducing greenhouse gas emissions, synthetic fuels can serve as an alternative to conventional fuels. Fossil fuel combustion remains one of the primary sources of anthropogenic CO_2 emissions and air pollution, underscoring the need to reduce its carbon footprint [9, 17]. In 2024, fossil fuels accounted for nearly 60% of the world's electricity generation [13]. In the transportation sector, up to 95% of the global transportation energy comes from petroleum-based liquid fuels, and by 2040, it is expected to represent between 80% and 90% [14]. Additionally, the stricter regulations on greenhouse gases (GHG) and exhaust emissions from internal combustion engines are meant to increase society's interest in improving the efficiency of combustion-based systems [26]. Among the viable alternatives to achieve this goal is by integrating renewable energy in the transport sector [9].

This integration is possible because hydrocarbons with similar chemical and physical properties to conventional fuels, called synthetic fuels, can be synthesized from the electrolysis of water and carbon dioxide captured from the air or industrial processes [7].

Synthetic fuels can be classified into one of the following categories: production process, feedstock, application, sustainability, or chemical composition [21]. Synthetic fuels derived from renewable electricity (through hydrogen generation in water electrolysis) and raw materials are called electro-fuels or e-fuels [26]. They are of special interest as they can be treated as a sustainable alternative to conventional fuels.

According to Uchida et al. [27], e-fuels can be produced with a chemical composition similar to that of conventional fuels, i.e. drop-in fuels for use in existing and next-generation engines, without significant design changes. However, some e-fuels can be substantially different, and they may require dedicated engines or new combustion concepts. According to the authors, these types of fuels are expected to accelerate the decarbonisation process.

Some processes to produce e-fuels include methanol-to-gasoline (MtG) for a gasoline surrogate, paraffinic fuels (Fischer-Tropsch FT process) for gasoline or Diesel; and polyoxymethylene dimethyl ethers (OMEx) representing a Diesel alternative [19, 27]. As a result of e-fuel production, for example, through the Fischer-Tropsch (FT) process, a mixture is formed that contains a wide range of chemical compounds, primarily consisting of olefins and paraffins with straight carbon chains [19]. Therefore, different chemical and physical properties of individual components in fuel mixtures influence the atomisation, mixture formation and combustion processes.

By implementing synthetic fuels, the carbon dioxide emissions related to their use are lower than the carbon dioxide captured during their production, resulting in a reduction of GHG emissions and achieving carbon-neutral or carbon-negative cycles when electrolysis is used with renewable energy [7]. Other benefits include the capability of utilising installed infrastructure for the storage and transportation of conventional fuels, as well as the possibility of extending the life cycle of current vehicles in operation. Reducing costs associated with developing specific infrastructure is a significant advantage, particularly in comparison to other technologies, such as battery or fuel cell electric vehicles [21].

As one may conclude, synthetic fuels can be identified as a viable alternative to conventional fuels within the transportation sector, with the benefit of reducing greenhouse gas and pollutant emissions. Moreover, their production could accomplish carbon-neutral or carbon-negative cycles. Additionally, the capability of using installed infrastructure facilitates their implementation compared to other technologies under investigation.

However, to facilitate the large-scale application of synthetic fuels, further research is still needed to determine optimal operating conditions, taking into account possibly different air-fuel mixture preparation processes. It needs to include possible flash-boiling, which has been previously shown to alter the atomisation and mixture formation processes.

Flash-boiling is a process related to the rapid phase change of the injected liquid, which may improve atomisation and mixture formation under internal conditions [4, 5]. It can be obtained by increasing the fuel temperature (prior to the injection) or by decreasing the ambient pressure (to which the liquid is injected) [1, 28].

The effects on the atomisation process due to flash-boiling are correlated with the saturation pressure of the injected liquid [4].

In general, a more complex relation is expected for multi-component fuels due to the different boiling points of each component, along with their varying molecular interactions. Furthermore, the saturation pressure curve for this type of mixture differs from that of pure components, exhibiting a dependence on molar fractions, pressure, and temperature. Fixing the molar fraction, the pressure-vs-temperature graph can be divided into two curves, the bubble curve and the dew curve, separated by the critical point [25]. Moreover, considering that the flash-boiling phenomenon is defined as a liquid being injected into an environment where the pressure is lower than the saturation pressure, causing superheating and violent evaporation, the bubble curve is crucial for understanding its behavior in multi-component fluids, as this line corresponds to the saturated liquid line. The dew curve, in turn, corresponds to the saturated vapour line.

Neroorkar and Schmidt [20] presented a model to determine the vapour-liquid equilibrium (VLE) characteristics of gasoline-ethanol blends, enabling flash-boiling injection simulations. The results obtained by the model were compared with experimental data and other previously validated models, exhibiting good agreement in the saturation pressure predictions for different ethanol contents. This pressure is used to determine the flash-boiling intensity through the ambient-to-saturation pressure ratio. Hutchison and Wallace [11] investigated the flash-boiling effect of surrogate and commercially available fuels on fuel volatility and particle emissions. The authors utilised the DWSIM chemical process simulation software to calculate the bubble point pressure of surrogate fuels at various temperatures, thereby determining the flash-boiling intensity. The numerical results obtained were validated with the dry vapour pressure (DVPE) experimental results.

Zeng et al. [29] used the ambient-to-saturation pressure ratio to identify three different regions: non-flash-boiling, transitional flash-boiling, and flare flash-boiling.

Xu et al. [28] evaluated flash-boiling characteristics for four different fuels, varying injection pressure, ambient pressure and fuel temperature. The authors presented a relationship between spray penetration and width, as well as the ambient-to-saturation pressure ratio and the air-to-liquid density ratio, under different flash-boiling regimes.

Hwang et al. [12] compared the spray characteristics of iso-octane with those of a multi-component gasoline surrogate under three different engine conditions: high density, flash-boiling, and early-injection conditions. Spray collapse was observed for the gasoline surrogate under flash-boiling and early-injection conditions, resulting in higher liquid and vapour spray penetration than iso-octane.

Kannaiyan and Sadr [15] compared the variation in spray parameters between two gas-to-liquid (GTL) synthetic fuels and Jet A-1 aviation fuel at injection pressures of 0.3 and 0.9 MPa. The results of the experiments show that there were no significant differences between the fuels in terms of the effective spray cone angle and global Sauter mean diameter (SMD). However, in the near nozzle region, especially at higher injection pressures, a variation in droplet velocity, Weber number (We), and mean droplet diameter (d_{10}), droplet disintegration and dispersion are identified. One of the reasons presented by the authors is related to differences in kinematic viscosity and surface tension between the fuels.

Cui et al. [8] compared the spray and combustion characteristics of methanol and *n*-heptane under subcooled and flash-boiling conditions. They used a two-hole injector, which operated under an injection pressure of 10 MPa. An increase in plume interference and spray angle, along with a reduction in unburned hydrocarbons, was observed for methanol under flash-boiling conditions.

Regarding the atomisation and vaporisation mechanisms of sprays under flash-boiling conditions, the following processes are defined: nucleation of bubbles, bubble growth, vaporisation, and droplet breakup [24]. Additionally, Robinson and Judd [22] defined four phases present in the bubble growth process: surface tension (ST), transition (T), inertia-controlled (IC), and heat transfer-controlled (HT).

Saha et al. [23] investigated the behaviour of a single droplet of oxymethylene ethers (OME_x) e-fuels under flash-boiling conditions, taking into account that, depending on the molecular characteristics of the e-fuels, their thermophysical characteristics present a considerable variation compared to conventional fuels. The authors reported that for OME_1 under low superheat conditions, only the surface tension and transition phases were observed in the bubble growth process; however, under moderate and high superheat conditions, the inertia-controlled phase was also observed. Finally, when comparing bubble growth between dimethyl ether (DME), OME_1 and OME_4, it was concluded that DME exhibited the fastest bubble growth rate.

Badawy et al. [3] evaluated the ambient-to-saturation pressure ratio reduction effect on the spray characteristics for four fuels (iso-octane, ethanol, methanol, and commercial grade gasoline). Although spray collapse was observed for all fuels at low ambient-to-saturation pressure ratios, no direct relationship was established with the variations observed in spray penetration, cone angle, axial velocity, and Sauter mean diameter.

Li et al. [18] investigated the impact of low ambient temperature on the spray characteristics of methanol by varying both ambient and fuel temperatures, demonstrating

that spray collapse under flash-boiling conditions is delayed when the ambient temperature is reduced.

Huang et al. [10] compared the spray characteristics (spray tip penetration and spray area) of gasoline and five synthetic fuels (ethanol-to-gasoline, G40, bio-naphtha, DMC, and bio-ethanol), under two different fuel temperatures, 25°C and 200°C. At 25°C, separation between the plumes was distinguished for all the fuels, but the ethanol-to-gasoline and bio-ethanol exhibited a higher penetration than the other fuels. At 200°C, bio-ethanol and G40 fuels presented the highest tip penetration. This study highlights the variations in spray morphology depending on the fuel; however, the impact of spray collapse on the final results was not addressed.

This study evaluates the morphological changes of synthetic fuel sprays when the flash-boiling conditions are reached. The analysis focused on comparing global spray structures and detecting a possible propensity for spray collapse. The bubble point calculation was performed following the approach presented by Hutchison and Wallace [11] for surrogate fuels. Experimental research on the injection and atomisation of a multi-component synthetic fuel under flash-boiling conditions was conducted using a constant-volume chamber and a high-speed camera.

2. Experimental setup

In the present research on the injection process of a synthetic fuel, a Bosch HDEV5.2 six-hole injector with a hole diameter of 0.35 mm was used. The injector was mounted in a constant volume chamber (CVC) with optical access. A round quartz window was placed in front of the camera to prevent fuel from splashing over the camera optics. As tests were performed only at an ambient pressure and temperature environment, the other side of the vessel was left open for easier operation. The back wall of the chamber (with respect to the camera) was covered with black material to decrease background scattering and improve the sharpness of the observed fuel spray.

Flash-boiling conditions were obtained by increasing the fluid temperature prior to the injection. The fuel temperature range was 25–120°C, and its upper value was limited by the injector's manufacturer-recommended operating temperature [6]. A constant injection pressure of 5 MPa was maintained in all tests.

Pressurisation of the system was based on a gas booster (Haskel, Single Acting – Single Stage model 86980), which increased the nitrogen pressure up to 5 MPa (gauge) pressure. The nitrogen pressure was monitored by a digital pressure gauge (Wika, model CPG1500).

To achieve refuelling at a controlled pressure and avoid air entrainment in the fuel line, a dedicated fuel line was implemented with an air-driven liquid pump (Maximator MSF111L). The nitrogen used to pressurise the fuel container was separated from the fuel by a piston designed and manufactured in stainless steel. It prevented nitrogen from dissolving in the fuel.

The injector opening time was set to 1.5 ms. The opening currents were set according to the manufacturer's specifications [6] at 9.4 A with a 704 μs pickup time and 3.4 A with a 696 μs hold-on time.

The injection process was recorded at a frequency of 20,000 frames per second using a Photron FastCam SA1.1 camera equipped with a Nikon AF NIKKOR 24–85 mm 1:2.8-4 D lens, with the aperture fully open. To ensure adequate illumination, the chamber was illuminated by two LED lamps (Amaran 200D) operating at full power and fitted with Fresnel lenses. A photograph of the experimental setup presenting its main components is shown in Fig. 1.
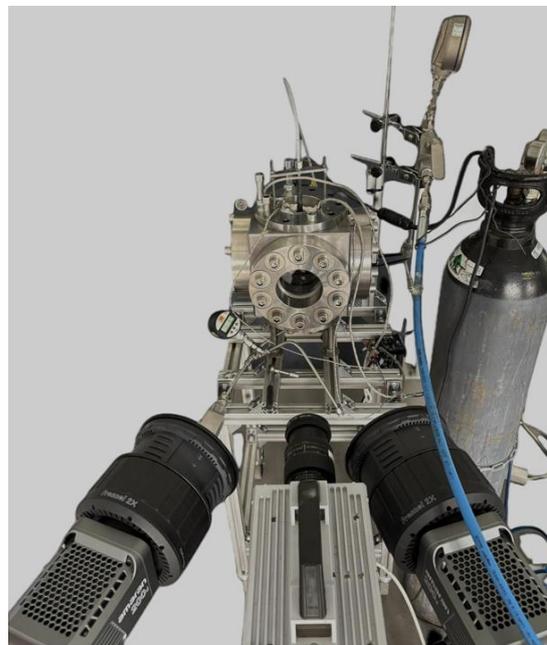

Fig. 1. Experimental setup – a photograph presenting main components: a constant volume chamber, high-speed camera and LED lamps (with Fresnel lens)

Figure 2 illustrates the arrangement of the setup and the interaction between its components.
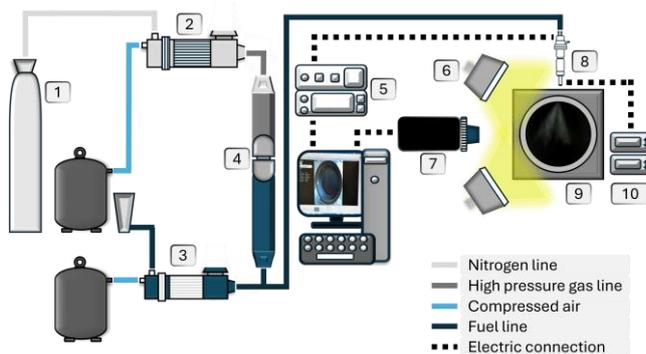

Fig. 2. Experimental setup: 1 – nitrogen tank, 2 – gas booster, 3 – fuel pump, 4 – piston, 5 – injection control unit, 6 – LED lamp, 7 – high-speed camera, 8 – injector, 9 – constant volume chamber, 10 – electric heater PID control

Image capture was performed using dedicated software provided by Photron, specifically PFV 4.4. The image recorded by the camera had a resolution of 564 × 564 pixels, and the injector was positioned so that its tip was visible within the camera's field of view.

The fuel temperature was controlled using two electric heaters connected to PID controllers, based on the indica-

tion from two J-type thermocouples. The injector temperature was set according to the calibration performed previously for the high-boiling-point silicone oil [2]. The uncertainty of the temperature measurement and control system's components is shown in Table 1.

Table 1. Temperature control system's components

Component	Uncertainty
Dewetron EPAD2	±0.3℃
EMS-3710 N (j-type thermocouple input)	±1℃

To study the structural and physical effects of flash-boiling, a synthetic fuel composition is presented in Table 2. *n*-heptane, toluene, and *n*-octane, as the main components, are used to study the flash-boiling structural and physical effects in multi-component synthetic fuels.

Table 2. Fuel composition

Component	Volume fraction [%]
n-heptane	40
n-octane	40
toluene	10
n-hexane	6
ethylbenzene	2
m-xylene	2

The density and viscosity of the synthetic fuel were 722–730 $\frac{kg}{m^3}$ at 15℃ and 0.45 mPa · s at 40℃, respectively.

In this study, similar to previous research [16], an inverse parameter (called the superheat index factor) is used instead of the ambient-to-saturation pressure ratio to describe the potential flash-boiling intensity. The superheat index factor R_p, is defined as the ratio of the saturation pressure P_{sat} for a given liquid temperature T_l to the ambient pressure P_a.

$$R_p = \frac{P_{sat(T_l)}}{P_a} \qquad (1)$$

Following the methodology from Hutchison and Wallace [11], the R_p ratio was evaluated using an ambient pressure 0.1 MPa and the saturation vapour pressure of the liquid as the bubble pressure for each liquid temperature T_l.

The bubble pressure curve was evaluated using the Soave-Redlich-Kwong equation of state, also implemented in the DWSIM software, which proved to be sufficiently accurate for describing the bubble pressure curve when compared to the validated results from UNIFAC-NIST bubble points. Table 3 and Fig. 3 summarise the R_p results.

Table 3. Fuel temperature, saturation pressure, and the superheat index

T_l [℃]	P_{sat} [MPa]	R_P [-]
60	0.02	0.19
90	0.06	0.55
120	0.13	1.34

The parameter that varied between series of tests was the temperature of the injected liquid. The injector and heaters were thermally insulated using glass wool. The time

required to stabilise the liquid temperature inside the injector was experimentally determined to be 20 minutes. Subsequent test series were conducted at a stabilisation time of 30 minutes. Test within a single series (for the same temperature) were performed at intervals of 1 minute. The first test in each series was not considered in the analysis. The required temperature setpoint relative to the actual temperature of the injected liquid was previously determined through a calibration procedure.
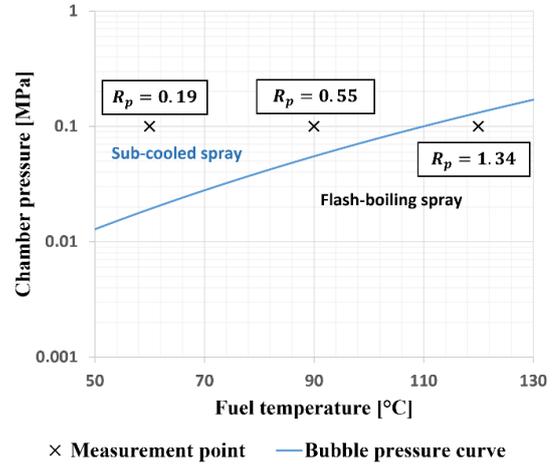

Fig. 3. Preheat ratio factor and flash-boiling regime

3. Results

The experimental investigation of the injection and atomisation of a synthetic fuel under subcooled and flash-boiling conditions provided detailed information on the dynamics of these processes. The studies performed using a multi-component surrogate synthetic fuel were focused on qualitative and quantitative analysis of the spray structures.

Figure 4 compares the selected spray images, after the background subtraction and the application of the artificial colour scale, with colours corresponding to the scattered light intensity detected by the camera pixels.

For the fuel temperatures 25℃ and 60℃, the differences between the spray clouds seem to be marginal, and it is observed for each considered time after the start of injection. As the fuel temperature increases from 25 to 120℃, an increase in the area covered by the spray becomes visible. Moreover, the scattering signal intensity along the spray axis and the spray area increased. At a fuel temperature of 120℃, initially separated regions of the spray cloud begin to merge, and the separation distance between the plumes is reduced. On this basis, it can be stated that at a temperature of 120℃, the individual plumes become wider due to rapid vaporization, which intensifies the breakup of the liquid jet and promotes finer droplet detachment with an increased radial-to-axial momentum ratio. However, the effects of flash-boiling, in this case, are not profound.

The spray structures were also evaluated quantitatively. For this purpose, three parameters were selected: spray tip penetration (STP), spray area, and spray width. The definition of STP, maximum width, and maximum area are presented in Fig. 5.

In Figure 5a, spray tip penetration, considered a macro parameter, is defined as the maximum distance reached by the fuel spray within the chamber. The maximum width parameter represents the maximum horizontal extent of the spray, defined as its overall width. The spray area refers to the largest area covered by the fuel (white colour) visible in Fig. 5b.
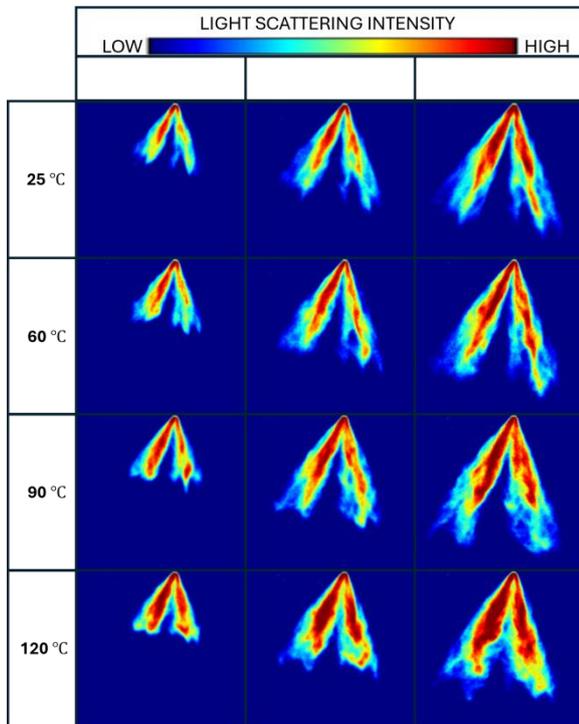

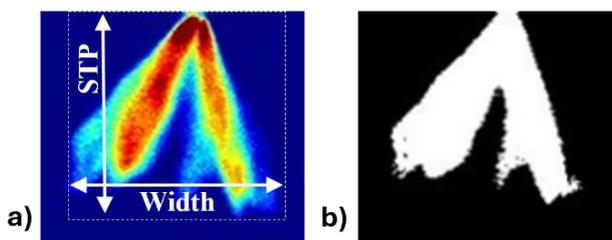Fig. 4. Spray clouds at 0.5, 1.0, and 1.5 ms after start of injection (ASOI) at varying fuel temperature

Fig. 5. Definition of: a) STP and spray width, b) spray area (white pixels)

Figures 6–8 present the results of spray tip penetration (STP), spray area, and spray width, respectively, for selected time points.

According to the results, the STP, spray area, and spray width measured for the multi-component synthetic fuel depend on the fuel temperature. The biggest differences were observed at 1.5 ms after the start of injection (ASOI). Heating fuel up to 120℃ leads to considerable changes in the macro parameters of the spray. After full development of the fuel sprays (1.5 ms), the highest STP was observed for fuel temperatures of 90 and 60℃. For fuel at 120℃, the STP is slightly smaller; the spray area and maximum width of the fuel spray are the largest compared to those at other temperatures.
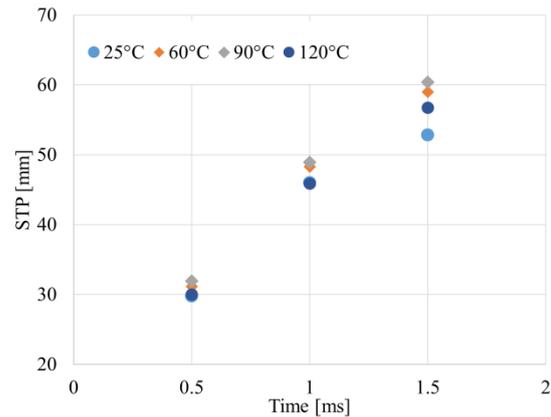

Fig. 6. Spray tip penetration of fuel spray at 0.5, 1.0, and 1.5 ms after start of injection
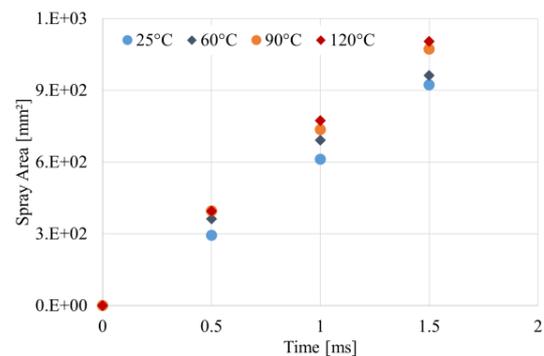

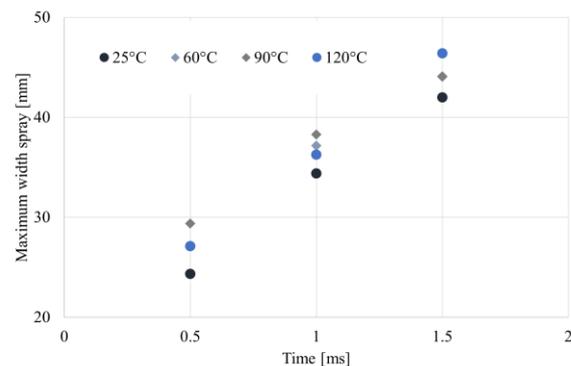Fig. 7. Spray area at 0.5, 1.0, and 1.5 ms after start of injection

Fig. 8. Maximum spray width at 0.5, 1.0, and 1.5 ms after start of injection

Both qualitative and quantitative analyses reveal the differences between the spray structures, suggesting possible effects from flash-boiling. The reduced spray tip penetration, increased spray area and width, as well as the reduced separation distance between the individual spray plumes, are in accordance with the flash-boiling effects observed by other researchers.

This agreement enables linking the observed changes with the rapid vaporisation, which intensifies the breakup of the liquid jet and promotes the formation of smaller droplets with an increased radial-to-axial momentum ratio. However, as the observed changes in the spray structures were not substantial, it is necessary to consider that other factors, such as reduced surface tension and viscosity, may also play a role.

4. Summary and conclusions

This paper presents the results of experimental studies of multi-component synthetic fuel sprays formed under flash-boiling conditions. The experimental studies were carried out on a dedicated test stand equipped with a multi-hole injector, a constant-volume chamber, and a high-speed camera used to visualise the sprays forms inside the constant-volume chamber. The acquired images were used to compare the spray structures in both qualitative and quantitative manners, and to draw conclusions about the possible effect of flash-boiling on the injection and atomisation of the considered synthetic fuel.

The results showed that the spray structure was sensitive to temperature changes, especially in the highest range (from 90 to 120°C), possibly resulting in flash-boiling. However, the secondary effects related to the rapid vaporisation of the injected fuel, in the form of spray collapse, were not observed, and the changes were not profound.

In general, the key observations related to the changes in spray morphology can be summarised as follows:

- At the highest studied temperature (120°C), the spray area and the scattering signal intensity visibly increased, suggesting enhanced atomisation and smaller droplets
- The individual plumes became thicker, and the separation distance between them decreased. Nevertheless, the plume separation was still observed even for the highest studied temperature
- The highest STP was observed for fuel temperatures of 60 and 90°C, under subcooled conditions
- Under flash-boiling conditions (120°C) and after full development of multi-component synthetic fuel sprays (1.5 ms), the spray tip penetration STP was slightly reduced. In contrast, the spray area and spray width were increased compared to other fuel temperatures.

All those observations suggest an effect of flash-boiling, even though the superheat index R_p was relatively low (1.34). However, the observed changes were not substantial, and the plume separation, visible even at the highest temperature, indicates that no significant near-nozzle effects from flash-boiling were present.

Nevertheless, in terms of possible cross-flowing air in an engine combustion chamber, even those small effects could influence the mixture formation, as smaller droplets, due to the increased importance of aerodynamic drag, exchange momentum with the ambient gas more effectively.

These aspects, in turn, suggest two important possible next steps in further research. Firstly, further studies are required to determine whether a further reduction in plume separation and spray collapse can be observed at lower ambient pressures (and increased superheat index) for this fuel. The second research could be oriented on the possible cross-flow effects on the altered sprays. Even slightly modified sprays can interact differently with the cross-flowing air. Such changes, in turn, could profoundly affect spray evolution in a combustion chamber, influencing the performance of the combustion process and engine emissions.

Acknowledgements

Nomenclature

ASOI	after start of injection	MtG	methanol-to-gasoline
CVC	constant volume chamber	OMEx	polyoxymethylene dimethyl ethers
d_{10}	mean droplet diameter	R_p	superheat index
DME	dimethyl ether	SMD	Sauter mean diameter
DVPE	dry vapour pressure equivalent	STP	spray tip penetration
FT	Fischer-Tropsch	TD	thermal-diffusion controlled
G-E	gasoline – ethanol	T_l	liquid temperature
GHG	greenhouse gases	VLE	vapour-liquid equilibrium
GTL	gas-to-liquid	W_e	Weber number
IC	inertia-controlled		

Bibliography

[1] Atac OF, Moon S, Jeon J. Unraveling the initial flash boiling spray formation at the same superheated index achieved by altering ambient pressure and fuel temperature independently. Int J Heat Mass Transf. 2021;169:120897. https://doi.org/10.1016/j.ijheatmasstransfer.2020.120897

[2] Bachanek J, Rogóż R, Pachler K, Tatschl R, Teodorczyk A, Kapusta ŁJ. Experimental study and empirical modelling of direct-injection n-heptane sprays formed under flash-boiling conditions. Int J Heat Mass Transf. 2025;236:126282. https://doi.org/10.1016/j.ijheatmasstransfer.2024.126282

[3] Badawy T, Xu H, Li Y. Macroscopic spray characteristics of iso-octane, ethanol, gasoline and methanol from a multi-hole injector under flash boiling conditions. Fuel. 2022;307: 121820. https://doi.org/10.1016/j.fuel.2021.121820

[4] Bar-Kohany T, Arogeti M, Malka A, Sher E. Advances in liquid atomization via flash boiling – a global overview. Energies. 2023;16(19):6763. https://doi.org/10.3390/en16196763

[5] Bar-Kohany T, Levy M. State of the art review of flash-boiling atomization. At Sprays. 2016;26(12):1259-1305. https://doi.org/10.1615/atomizspr.2016015626

[6] Bosch Motorsport. HP Injection Valve HDEV 5.2. https://www.bosch-motorsport.com/content/downloads/Raceparts/en-GB/49510539208591115.html#/Tabs=9007199304263179/

[7] Cremades LV., Oller L. Techno-environmental feasibility of synthetic fuels in ground transportation. Application to the Spanish automobile fleet in 2035. Energy Reports. 2024;11: 5466-5474. https://doi.org/10.1016/j.egyr.2024.05.032

[8] Cui M, Nour M, Fu J, Zhang W, Wang G, Xu H, et al. Fundamental investigation of methanol flash boiling combustion under direct injection conditions. Combust Flame. 2025;276. https://doi.org/10.1016/j.combustflame.2025.114147

[9] Deutz S, Bongartz D, Heuser B, Kätelhön A, Schulze Langenhorst L, Omari A et al. Cleaner production of cleaner fuels: Wind-to-wheel-environmental assessment of CO2-based oxymethylene ether as a drop-in fuel. Energy Environ Sci. 2018;11(2):331-343. https://doi.org/10.1039/c7ee01657c

[10] Huang W, Oguma M, Kinoshita K, Abe Y, Tanaka K. Investigating spray characteristics of synthetic fuels: comparative analysis with gasoline. Int J Automot Manuf Mater. 2024;2-2. https://doi.org/10.53941/ijamm.2024.100008

[11] Hutchison BRM, Wallace JS. Influence of fuel volatility on particulate matter emissions from a production DISI engine. Fuel. 2021;303:121206. https://doi.org/10.1016/j.fuel.2021.121206

[12] Hwang J, Karathanassis IK, Koukouvinis P, Nguyen T, Tagliante F, Pickett LM et al. Spray process of multicomponent gasoline surrogate fuel under ECN Spray G conditions. Int J Multiph Flow. 2024;174:104753. https://doi.org/10.1016/j.ijmultiphaseflow.2024.104753

[13] International Energy Agency. Global Energy Review 2025 – Natural Gas. 2025. https://www.iea.org/reports/global-energy-review-2025/global-trends

[14] Kalghatgi G, Agarwal AK, Senecal K, Leach F. Introduction to engines and fuels for future transport. Energy, Environment, and Sustainability. 2022:1-5. https://doi.org/10.1007/978-981-16-8717-4_1

[15] Kannaiyan K, Sadr R. Experimental investigation of spray characteristics of alternative aviation fuels. Energy Convers Manag. 2014;88:1060-1069. https://doi.org/10.1016/j.enconman.2014.09.037

[16] Kapusta ŁJ. Understanding the collapse of flash-boiling sprays formed by multi-hole injectors operating at low injection pressures. Energy. 2022;247:123388. https://doi.org/10.1016/j.energy.2022.123388

[17] Letcher TM. Introduction with a focus on atmospheric carbon dioxide and climate change. Future Energy: Improved. Sustainable and Clean Options for Our Planet. 2020:3-17. https://doi.org/10.1016/b978-0-08-102886-5.00001-3

[18] Li X, Xiang L, Wang L, Wang Z, Hu Y. Experimental study on macroscopic and microscopic characteristics of flash boiling methanol spray under extremely cold conditions. Energy Convers Manag. 2025;333:119780. https://doi.org/10.1016/j.enconman.2025.119780

[19] Liu G, Larson ED. Comparison of coal/biomass co-processing systems with CCS for production of low-carbon synthetic fuels: methanol-to-gasoline and Fischer-Tropsch. Energy Procedia. 2014:7315-7329. https://doi.org/10.1016/j.egypro.2014.11.768

[20] Neroorkar K, Schmidt D. Modeling of vapor-liquid equilibrium of gasoline-ethanol blended fuels for flash boiling simulations. Fuel. 2011;90(2):665-673. https://doi.org/10.1016/j.fuel.2010.09.035

[21] Ram V, Salkuti SR. An overview of major synthetic fuels. Energies. 2023:16. https://doi.org/10.3390/en16062834

[22] Robinson AJ, Judd RL. Bubble growth in a uniform and spatially distributed temperature field. Int J Heat Mass Transf. 2001;44(14):2699-2710. https://doi.org/10.1016/S0017-9310(00)00294-5

[23] Saha A, Grenga T, Deshmukh AY, Hinrichs J, Bode M, Pitsch H. Numerical modeling of single droplet flash boiling behavior of e-fuels considering internal and external vaporization. Fuel. 2022;308:121934. https://doi.org/10.1016/j.fuel.2021.121934

[24] Senda J, Hojyo Y, Fujimoto H. Modeling on atomization and vaporization process in flash boiling spray. JSAE Rev. 1994;15(4):291-296. https://doi.org/10.1016/0389-4304(94)90209-7

[25] Smith JM, Ness HC Van, Abbott MM, Swihart MT. Introduction to chemical engineering thermodynamics eighth edition. 8 ed. New York: McGraw-Hill 2018:68-132.

[26] Stępień Z. Synthetic automotive fuels. Combustion Engines. 2023;192(1):78-90. https://doi.org/10.19206/CE-152526

[27] Uchida N, Onorati A, Novella R, Agarwal AK, Abdul-Manan AFN, Kulzer AC et al. E-fuels in IC engines: a key solution for a future decarbonized transport. Int J Eng Res. 2025. https://doi.org/10.1177/14680874251325296

[28] Xu M, Zhang Y, Zeng W, Zhang G, Zhang M. Flash boiling: easy and better way to generate ideal sprays than the high injection pressure. SAE Int J Fuels Lubr. 2013;6(1):137-148. https://doi.org/10.4271/2013-01-1614

[29] Zeng W, Xu M, Zhang G, Zhang Y, Cleary DJ. Atomization and vaporization for flash-boiling multi-hole sprays with alcohol fuels. Fuel. 2012;95:287-297. https://doi.org/10.1016/j.fuel.2011.08.048

Henry Andrés Porras Perucho, MSc. – Faculty of Power and Aeronautical Engineering, Warsaw University of Technology, Poland.
e-mail: *henry.porras_perucho.dokt@pw.edu.pl*

Joanna Grochowalska, DEng. – Faculty of Mechanical Engineering and Ship Technology, Gdańsk University of Technology, Poland.
e-mail: *joanna.grochowalska@pg.edu.pl*

Cláudio Manuel Vianna Moreira, BSc. – Faculty of Sciences, Physics Department, University of Lisbon, Portugal.
e-mail: *claumvmoreira@gmail.com*

Łukasz Jan Kapusta, DEng. – Faculty of Power and Aeronautical Engineering, Warsaw University of Technology, Poland.
e-mail: *lukasz.kapusta@pw.edu.pl*

Łukasz Boruc, DEng. – Faculty of Power and Aeronautical Engineering, Warsaw University of Technology, Poland.
e-mail: *lukasz.boruc@pw.edu.pl*